Exciton transport by nonequilibrium phonons and its effect on recombination radiation from semiconductors at high excitation levels

N. N. Zinov'ev, L. P. Ivanov, V. I. Kozub, and I. D. Yaroshetskiĭ

A. F. Ioffe Physicotechnical Institute, USSR Academy of Sciences
(Submitted 22 July 1982)
Zh. Eksp. Teor. Fiz. **84**, 1761–1780 (May 1983)

We investigated the observed transport of excitons in semiconductors (CdS). We demonstrate experimentally and theoretically that the observed exciton drift can be due to their dragging by a stream of nonequilibrium acoustic phonons. The transport of the excitons by phonons is investigated and the main characteristics of this phenomenon are determined both in the case of a semiconductor excited by strongly absorbed light (the nonequilibrium phonons are produced in this case as a result of thermalization and nonradiative recombination of the generated electron-hole pairs), and as a result of injection of phonons into the sample by heating a metallic film sputtered over the surface of the semiconductor.

PACS numbers: 71.35. + z, 72.10.Di

Increasing the excitation level produces in the spectra of the recombination radiation of direct-band (II–VI, III-V) semiconductors considerable changes, which were interpreted in a number of studies as manifestations of collective interactions in a system of nonequilibrium electron-hole pairs (NEHP) of high density.[1]

There exist at present several viewpoints concerning the nature of the produced emission lines.[1–8] It is important to note that in the analysis of recombination-radiation spectra at high excitation levels it is necessary to take into account the transport processes in the NEHP system. Phenomena of this kind were first discussed in Ref. 9 as applied to the case of electron-hole pairs in Ge at helium temperatures. Attention was called there to the possibility of transport of the electron-hole drops (EHD) by the nonequilibrium phonons produced in the course of relaxation of the NEHP and propagating ballistically in the sample (the so called phonon wind).

In our preceding investigations[8,10] we observed a change in the character of the recombination of the free excitons (FE) at $T > 40$ K. This change manifests itself both in a modification of the emission line from the resonant state,[8] and in an anomalous increase of the luminescence intensity on the FE–LO phonon replica lines relative to the zero-phonon emission line of the exciton.[8,10a] It was observed in Ref. 10a that at high surface excitation intensities a drift transport of the electrons takes place. It was suggested in the same reference that the possible mechanism of this transport is the dragging of the FE by a stream of nonequilibrium phonons produced in the sub-surface layer of the crystal. We note that as applied to the case of the FE this phenomenon was investigated for the first time.

In the present paper we report a systematic investigation of the drift transport of FE in CdS crystals at $T > 40$ K. It will be shown that the physical picture in this situation differs from that investigated in Ref. 9. This pertains both to the electron-hole system and (a particularly important factor) to the phonon system, inasmuch as in the case considered we are dealing with a region of sufficiently high temperatures, when the phonon-phonon scattering (including that with umklapp) plays a most important role.

The plan of the exposition is the following. In Sec. 1 we describe, the experimental procedure; in Sec 2 are given the results of an experimental investigation of exciton motion using optical methods of observation; alternate mechanisms of increasing the size of the region occupied by the excitons are discussed. In Sec. 3 we present a theoretical analysis of the phonon system of a semiconductor under the conditions of the perturbation produced by phonon generation upon recombination and thermalization of the NEHP; the exciton dragging due to this perturbation is analyzed. In Sec. 4 we discuss the results and compare the experimental data with the deductions of the theory.

1. EXPERIMENTAL PROCEDURE

The object of the investigations was the II-VI semiconductor cadmium sulfide. Samples grown from the gas phase had a residual-donor density $N_D \lesssim 10^{15}$ cm^{-3}. Typical sample sizes were 3×6 mm, at thickness 10–40 μm. The hexagonal c axis of the crystal was in the plane of the plate. The recombination radiation of the crystal was excited by light from an N_2 laser with pulse duration $t_0 = 5 \times 10^{-9}$ and 10^{-8} sec, power up to 500 kW, and repetition frequency up to 90 Hz. The recombination-radiation spectra were analyzed in two geometries: in transmission ($\mathbf{k}_I \| \mathbf{k}_L$) and in reflection ($\mathbf{k}_I \| \sim -\mathbf{k}_L$) ($\mathbf{k}_I$ and $\mathbf{k}_L$ are the respective wave vectors of the exciting and recombination radiation). The spectral instrument was a DFS-24 monochromator. The spectral width of the slit of the monochromator did not exceed in any case 10^{-3} eV. The luminescence polarization was analyzed in accordance with the known selection rules for CdS crystals. The luminescence signal was recorded with a high-speed photomultiplier and a stroboscopic signal-recording system. The recording system displayed without distortion a light pulse of front duration $\sim 10^{-9}$ sec. The samples were placed in the chamber of a controlled-temperature cryostat; the experiments were performed in the temperature range $30 < T < 130$ K. The temperature was maintained constant within ~ 0.01 K. To prevent a possible influence of the sti-

 0038-5646/83/051027-11$04.00

mulated emission on the luminescence spectra, the laser beam was focused into a spot of 50 μm diameter. The monochromator analyzed the central region of the excitation spot, which was separated with special masks and diaphragms. In addition, we investigated the modification of the recombination-radiation spectrum by a change in the size of the excitation region—this revealed the influence of stimulated emission on the recorded spectrum. The range of the employed excitation intensities was bounded from above by the pump intensity at which the stimulated emission first appeared. The exciton lifetime was measured using two-photon volume excitation of the sample by the second harmonic of an YAG-Nd$^+$ laser ($\lambda = 0.53$ μm) with pulse duration 12×10^{-9} sec. The diffusion coefficient of the free excitons in the investigated CdS sample was determined by the method described in Ref. 10b.

To investigate the influence of the flux of nonequilibrium phonons on the exciton system we used a set of samples with a metallic film (In, Au) of thickness $\approx$200 Å sputtered on part of a crystal surface. Simultaneously with the sputtering of the metal on the semiconductor, a metallic layer of the same thickness was sputtered on part of the surface of a thin quartz plate, which served as a special filter to attenuate the exciting radiation by the same amount as the metal layer on the crystal surface. The joint use of the filter and of the sample with metallic film made it possible, while maintaining the density of the generated excitons constant, to vary the intensity of the phonon flux (Sec. 2). The equality of attenuation of the exciting radiation by the metal layers on the quartz glass and on the sample was additionally monitored by the behavior of the spectral composition of the FE luminescence at weak pump intensities (< 1W/cm^2), and by the transparency of the filter and of the sample to helium-neon laser radiation.

2. KINETICS OF RECOMBINATION RADIATION OF A FREE EXCITON

Figure 1 shows the spectra of the recombination radiation in two observation geometries: in transmission ($\mathbf{k}_I \| \mathbf{k}_L$) and in reflection ($\mathbf{k}_I \| -\mathbf{k}_L$). It is seen that in the geometry with $\mathbf{k}_I \| -\mathbf{k}_L$ the intensity of the FE line decreases with increasing excitation intensity I relative to the FE–LO phonon replica line. We note that the crystal region in which the excitons are generated and the sample region from which the luminescence is observbed are spatially separated in the $\mathbf{k}_I \| \mathbf{k}_L$ geometry but are superimposed at $\mathbf{k}_I \cdot -\mathbf{k}_L$. Assuming an exciton diffusion coefficient $D \approx 6$ cm^2/sec (Ref. 10b) and an exciton lifetime $\tau \sim 10^{-9}$ sec, we find that the characteristic diffusion length is $L_D \sim 10^{-4}$ cm, whereas the distance between the region of exciton generation and the region of observation is the thickness of the sample $L \sim 10^{-3}$ cm, and consequently $L \gg L_D$. Thus, the usual diffusion penetration of the excitons over a distance L is not very effective. What is significant is a feature peculiar to direct-band semiconductor, namely the large value of the light abosrption coefficient on the FE line, where $\alpha_X \sim 10^5$ cm^{-1}, and its abrupt decrease near the fundamental-absorption edge, so that in the FE–LO region, where $\alpha_{X-LO} \sim 10^2$ cm^{-1}, the sample is practically transparent to the radiation in this spectral region. The foregoing circumstances enable us to detect the excitons, with high temporal resolution, by using the exciton emission on the FE line. Entry of the excitons into the "detector" region (the sample volume near the surface, with characteristic dimension $l_X \sim \alpha_X^{-1} \sim 10^{-5}$ cm) can then be revealed by the presence of emission on the FE line. On the other hand, emission on the FE–LO line yields information on the total number of excitons in the sample.

Figure 2 shows the dependences of the luminescence intensity of the FE and FE–LO lines on the excitation level in the two investigated geometries. It can be seen that the dependence of the intensity of the zero-phonon line of the FE luminescence in the lasing region ($\mathbf{k}_I \cdot -\mathbf{k}_L$) on I, starting with a certain excitation level, undergoes a transition from linear to sublinear with a tendency to saturation. At the same time, the intensity of the FE–LO recombination radiation continues to increase with practically linearly I. In turn, the intensity of the FE line emission in the detector ($\mathbf{k}_I \| \mathbf{k}_L$) increases superlinearly, starting approximately with the same value of the excitation at which the sublinear behavior appears in the $\mathbf{k}_I \| -\mathbf{k}_L$ geometry. Since luminescence intensity of the excitons is proportional to their density, the experimentally observed behavior of the recombination radiation offers evidence of the following.

1. In the NEHP generation region, the growth of the

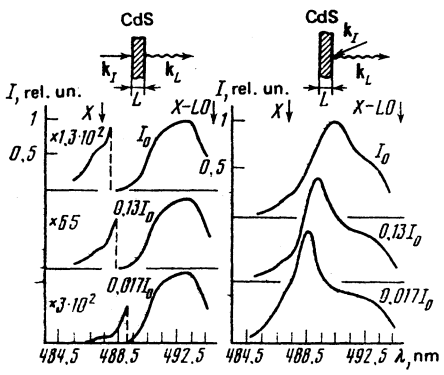

FIG. 1. Recombination-radiation spectra plotted in the geometry $\mathbf{k}_I \| \mathbf{k}_L$ and $\mathbf{k}_I \| -\mathbf{k}_L$, polarization E$\perp$c, $I_0 = 4\times10^{24}$ cm^{-2}·sec^{-1}, $T = 77$ K, $L = 2\times10^{-3}$ cm.

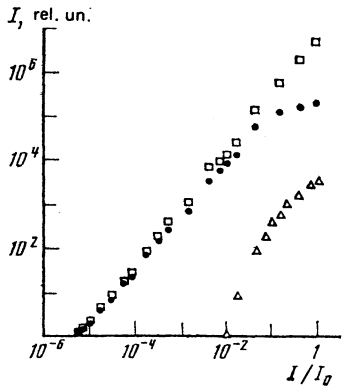

FIG. 2. Dependences of the luminescence intensity on the excitation I on the lines FE and FE–LO; $I_0 = 4\times10^{24}$ cm^{-2}·sec^{-1}, $T = 77$ K, $L = 2\times10^{-3}$ (□—$X - LO$, ●—$X(\mathbf{k}_I \| -\mathbf{k}_L$, △—$X(\mathbf{k}_I \| \mathbf{k}_L)$).

exciton density stabilizes with increasing I. 2. At a distance $x = L$ from the generation region, the density of the excitons increases superlinearly with increasing pump. 3. The number of excitons integrated over the volume increases linearly with increasing excitation intensity in the entire investigated pump range.

Thus, the foregoing results indicate that the excitons penetrate into the sample, with increasing excitation level, to distances that exceed considerably the diffusion length, i.e., the volume occupied by them increases with increasing excitation.

To analyze the character of the exciton motion we have investigated, at different values of I, the temporal evolution of the luminescence signal in the detector region, both in the geometry $\mathbf{k}_I \| -\mathbf{k}_L$ and in the geometry $\mathbf{k}_I \| \mathbf{k}_L$, when the regions of generation and detection of the FE are spatially separated. From an analysis of the experimental data we can draw the following conclusions (see Fig. 5 below).

First, substantial differences are observed in the temporal evolution of the exciton radiation from two spatially separated regions of the sample. The signal from the detector region ($\mathbf{k}_I \| \mathbf{k}_L$) undergoes changes typical of drift motion, namely, with increasing excitation intensity the excitons negotiate the distance L faster. This manifests itself in a characteristic shift of the maximum of the time dependence towards the instant of time $t = 0$ and to a decrease of the duration of the radiation pulse. At the same time, the shape of the FE line pulse from the region $x \approx 0 (\mathbf{k}_I \| -\mathbf{k}_L)$ remains practically unchanged when the pump is varied.

Second, as for the FE–LO line, experiment[8] shows that at very low intensities its temporal dependence duplicates in the main the shape of the laser pulse. An increase of I leads to a superlinear dependence of the signal at $t > t_0$, i.e., to the appearance of a slow component in the variation of the luminescence signal with time. In the case $I \gtrsim 10^{22}$ cm^{-2} sec^{-1}, the shape of the pulse ceases to depend on I, and the characteristic duration of the pulse is in this case noticeably longer than t_0. At the same time, the shape of the pulse on the FE line in the reflection geometry corresponds practically to the shape of the laser pulse. Recognizing that a contribution to the response on the FE lineis made only by excitons situated in a subsurface layer of thickness $\sim \alpha_X^{-1}$, while on the FE–LO line also by excitons in the volume, the data presented above offer evidence that the recombination of the FE behaves differently near the surface and in the volume. In this situation, modification of the signal on the FE–LO line with increasing I may be due to the fact that when I is increased the excitons penetrate, by drifting, into the sample, where their lifetime is long.[1)] The invariance of the shape of the pulse at sufficiently large I is evidence of invariance of the damping constant of the luminescence signal or of the lifetime of the excitons as functions of the excitation intensity. This is confirmed also by the fact cited above, that the luminescence intensity on the FE–LO line has a linear dependence on the pump.

It must be noted that the effects observed do not change when the position of the excitation spot on the surface of the crystal is changed, and also when the sample is rotated through 180°. This is evidence of sufficient identity of the sample surfaces, as well as of the absence of an influence of any local inhomogeneities on the experimental data.

Thus, the experimental results indicate not simply that the size of the exciton cloud increases with time, but that the excitons move by drifting, under the influence of a certain force that depends on the excitation intensity.

To explain this behavior we have invoked an idea, proposed in Ref. 9, that the excitons are dragged by the nonequilibrium phonons generated as a result of thermalization and nonradiative recombination of the NEHP in the thin subsurface layer of the sample. The experimental conditions in our case, however, as will be shown below, differ substantially from the situation corresponding to the EHD dragging investigated in Refs. 9, 11, and 12.

In principal, another transport mechanism is also possible, and depends on the light intensity, namely photostimulated diffusion.[13,14] This case, as shown in Refs. 13 and 14, the increment to the usual diffusion flux is given by

$$J = \langle \alpha^{-2} \rangle \int \frac{\partial R}{\partial x} dE,$$

where R is the rate of radiative recombination and E is the energy. It can be seen from this formula that the increment to the diffusion on account of photostimulated depends on the form of the radiative recombination (linear, quadratic, etc.). What is important, however, is that in the case of linear recombination (such as exciton recombination[15]) we obtain for the diffusion coefficient an increment that does not depend on the density of the particles in the system, i.e., on the excitation intensity, whereas in experiment one observes a substantial dependence n the pump. In the case of band-band recombination we have $R = \rho(E) B n^2 (\rho(E)$ is the probability of emission of a quantum of energy E, B is the radiative recombination coefficient and n is the carrier density), and then $D_{pd} \sim 5 \times 10^{-18} n$ (Ref. 14). At $\alpha \sim 10^4$ cm^{-1}, $B \gtrsim 7 \times 10^{-10}$ cm^{-3} we obtain $D \gtrsim 20$ cm^2/sec. It can thus be seen from the foregoing estimates that to realize photostimulated transport the necessary conditions are the following: the presence of nonlinear recombination, a value $\alpha \lesssim 10^4$ cm^{-1}, a sufficiently high coefficient of radiative recombination (the estimate given above for B is for GaAs crystals, which have an almost 100% internal quantum yield). As for excitons, the nonlinear process in such a system[2] should lead to the appearance of radiation in the region of frequencies where the absorption coefficients is $\sim 10^2$ cm^{-1}, i.e., the photon leaves the crystal without being absorbed. In the case of CdS, in which the exciton has a high binding energy (≈ 28 meV), the recombination is effected via exciton states, and it is impossible to observe in experiment the radiation corresponding to band-band recombination. Analysis shows that other possible effects that lead to an increase of the dimensions of the exciton cloud (transparentization, expansion due tothe mechanism considered in Ref. 16) do not play a significant role in our case.

Before we proceed to consider the phonon-system disequilibrium, its evolution, and the character of motion of excitons under the conditions of this disequilibrium, we dis-

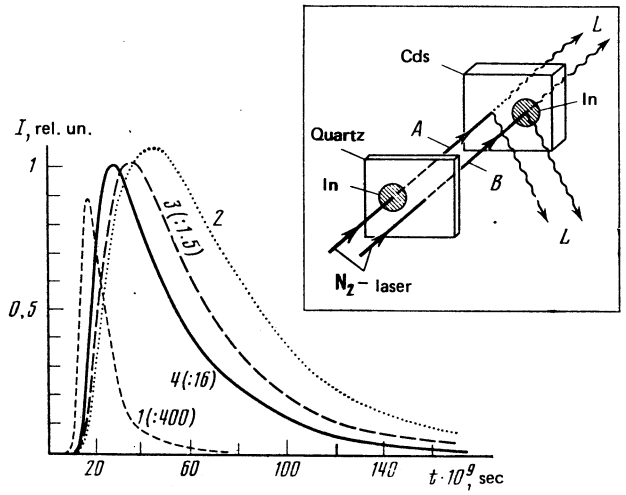

FIG. 3. Kinetics of recombination radiation of an exciton from the resonant state following the action of a thermal pulse: 1—shape of radiation pulse in the geometries $\mathbf{k}_I \| -\mathbf{k}_L$ (A) and (B); 2—shape of radiation pulse in the geometry $\mathbf{k}_I \| \mathbf{k}_L(A)$; 3—shape of radiation pulse in the geometry $\mathbf{k}_I \| \mathbf{k}_L(B)$; 4—shape of radiation pulse in the geometry $\mathbf{k}_I \| \mathbf{k}_L$ for excitation of the bare surface of the sample with light of intensity $I = I_B (T = 77$ K, $L = 2\times 10^{-3}$ cm).

cuss the results of experiments on the interaction of excitons with a thermal pulse (cf. Ref. 17). We have performed the following experiment (insets in Figs. 3 and 4). A thin layer ($\approx$200 Å) of metal (In, Au) was sputtered on the surface of a CdS sample. Simultaneously, a special filter was prepared and placed in front of the sample and making no contact with it, so as to be able to decrease the intensity of the light by as much as it is attenuated by the indicated metallic film (approximately 10 times). In channel A the light passes through the filter and is incident on the free surface of the sample, while in channel B the light is incident on the metallic film located directly on the surface of the sample. In accordance with the foregoing, the intensity of the light passing in the CdS and producing excitons should be the same in both channels; consequently the density of the produced excitons should also be the same. However, whereas the absorption of the light by the filter in channel A does not heat the sample, the power absorbed in the metallic film in channel B leads to generation of a phonon flux that penetrates into the sample. As a result, the intensity of the phonon flux in channel B is approximately 10 times larger than the corresponding intensity in channel A. Figures 3 and 4 show the results of this experiment. It can be seen from Fig. 4 (curve 1) that deposition of a metallic film does not influence significantly the luminescence at low excitation intensities and the spectra in the case of excitation of bare surface of the crystal and a surface coated with a thin layer of metal practically coincide. We investigated the spectra (Fig. 4) and the temporal kinetics of exciton radiation in the two considered geometries. As can be seen from Figs. 3 and 4, when an additional phonon flux is generated (curve 3 of Fig. 3) the temporal kinetics in the detector (from the region $x = L$) changes qualitatively in the same manner as in the case shown in Fig. 5, namely, the excitons negotiate the distance L more rapidly with increasing I and the exciton packet spreads out less as a result of diffusion. A comparison of curves 4 and 3 of Fig. 3 we can see that dragging by the thermal pulse is less effective than excitation of the superconductor by light of the same intensity. We note also that the same number of excitons is produced in cases A and B, as confirmed by the invariance of the area under the curve on going from 2 to 3 in Fig. 3. It can also be seen that the intensity of the FE line decreases substantially following the action of a thermal pulse; this is evidence of additional departure of part of the excitons from the sample subsurface into the volume.

The results of the reported experiments confirm the foregoing assumption of drift motion of the excitons and phonon dragging mechanism.

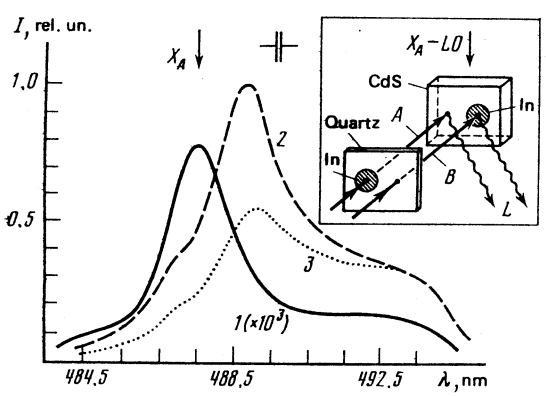

FIG. 4. Recombination radiation spectra of FE following the action of phonons of a thermal pulse: 1—excitation intensity $I = 10^{18}$–10^{19} cm^{-2}·sec^{-1}; 2—excitation intensity $I = I_A = 3\times 10^{23}$cm^{-2}·sec^{-1}; 3—excitation intensity $I = I_B = 3\times 10^{24}$ cm^{-2}·sec^{-3}; observation geometry in 1, 2, and 3: $\mathbf{k}_I \| -\mathbf{k}_L$, $T = 77$ K, $L = 2\times 10^{-3}$ cm.

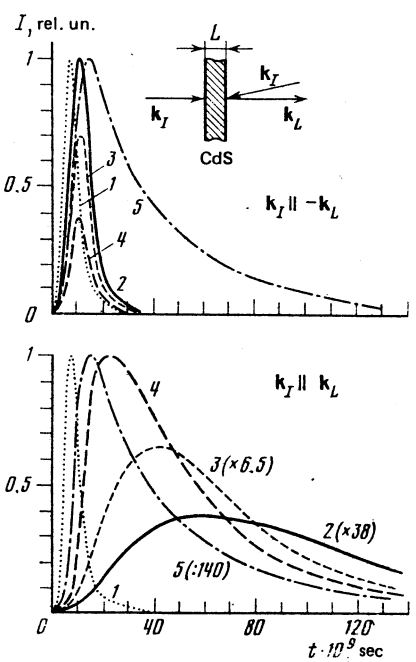

FIG. 5. Kinetics of luminescence in the geometries $\mathbf{k}_I \| -\mathbf{k}_L$ and $\mathbf{k}_I \| \mathbf{k}_L$, $T = 77$ K, $L = 2\times 10^{-3}$ cm 1—shape of excitation pulse; shape of FE radiation pulse at: 2—$I = 1.2\times 10^{23}$ cm^{-2}·sec^{-1}; 5—shape of radiation pulse of phonon replica of FE at $I = 5\times 10^{21}$–4×10^{24} cm^{-2}·sec^{-1}.

3. PROPAGATION OF NONEQUILIBRIUM PHONONS AND EXCITON DRAGGING (THEORY)

We start with an analysis of the processes that occur in the phonon system. The cause of the system disequilibrium is relaxation of the NEHP generated by the laser radiation, a relaxation accompanied by emission of a large number of phonons, for the most part optical. The characteristic times of emission of an optical phonon by a carrier amount in this case to $\sim 10^{-13}$ sec, and the corresponding range is $\sim 10^{-6}$ cm. Thus, the phonon-production region is localized near the front surface of the sample $x = 0$ (the x axis is normal to the surface of the film) at distances of the order of the damping length of the exciting light, $\sim 10^{-5}$ cm. The next stage is the decay of optical phonons into acoustic ones and also takes place within short times, $\sim 10^{-11}$ sec. Very important for the subsequent relaxation in the phonon system is that in the considered temperature region (above 40 K) three-phonon processes with participation of thermal phonons are the effective ones. Thus, at $T \approx 77$ K we have for the characteristic time of normal three-phonon processes, in the case of phonons with energies $\hbar\omega \sim T$, the estimate[18] $\tau_N \sim (T^5/\rho\hbar^4\bar{w}^5)^{-1} \sim 0.5 \times 10^{-10}$ sec (here ρ is the density of the crystal and $\bar{w}$ is the average speed of sound); the corresponding mean path is $l_N \sim 10^{-5}$ cm. As a result, over times longer than τ_N and over distances more than 10^{-5} cm from the surface, most nonequilibrium phonons are thermalized, and the disequilibrium for them manifests itself as inhomogeneity of the distribution of the local temperature. Moreover, in this temperature region there occur also effectively three-phonon processes with umklapp, since the parameter $\Theta/T \sim 5$ (Θ is the Debye temperature) is not too large and the exponential smallness of $\exp(-\Theta/T)$ is offset by the corresponding increase of the phase volume. These considerations agree with the experimental estimate of the total relaxation time of phonons in CdS, which takes into account different processes[19] and is obtained from an analysis of the thermal conductivity:

$$\tau^{-1} = A\omega^4 + [B_1 + B_2 \exp(-\Theta/\alpha T)]\omega^2 T^3, \qquad (1)$$

where the coefficient A, which describes the scattering by defects, does not exceed 10^{-43} sec^3 for sufficiently pure samples; $B_1 \approx 1.4 \times 10^{-22}$ sec/deg^3, $B_2 \approx 3.8 \times 10^{-21}$ sec/deg^3 (B_1 and B_2 are connected respectively with N and U processes), and $\alpha \approx 1$–9. In accordance with (1) at $\hbar\omega \sim T \approx 77$ K we have $\tau_N \sim \tau_U \sim 10^{-10}$ sec. Thus, the thermal-phonon mean free path for processes with umklapp is $\sim 10^{-5}$ cm, and consequently the change of the temperature over the characteristic scales of the experiment ($\sim 10^{-3}$ cm) is due to ordinary thermal conductivity.

This behavior, due primarily to the contribution of the attachment of equilibrium thermal phonons, distinguishes essentially the present situation from that typical of experiments on dragging of EHD by phonon wind and considered in Ref. 9. The latter corresponded to the region of low near-helium temperatures, when the main processes in the phonon system are decay processes.

From the conservation laws, however, it follows that only phonons with low energies $\hbar\omega \ll T$ can interact with excitons. Indeed, the condition $\hbar\theta \leqslant \bar{p}$ must be satisfied, where $\hbar q$ is the phonon momentum and $\bar{p}$ is the characteristic momentum of the exciton. From this we get the estimate $\hbar\omega/T \leqslant w/\bar{v}$, where w is the phonon velocity and $\bar{v}$ is the thermal velocity of the exciton. From theoretical estimates, and also from the experimental estimate (1), it follows that the characteristic relaxation time τ_* of these long-wave phonons turns out to be larger by $(v/w)^2$ times than for thermal phonons, and at $T \sim 80$ K it is of the order of 10^{-8} sec. The mean free path l_* for them is correspondingly of the order of 10^{-3} cm, i.e., of the order of the sample thickness. Consequently, the excitons interact with phonons that propagate almost ballistically. We note that the principal relaxation mechanism in this group of phonons is the joining together of thermal phonons; this ensures relaxation of both the energy and of the momentum of this group. Another possible momentum relaxation mechanism is diffuse scattering by the sample boundaries.

Despite the large mean free paths of the long-wave phonons, their relative contribution to the heat transfer is small ($l_* \propto q^{-2}$ as against a state density $\propto q^2$). An important circumstance here, in particular, is also that under the experimental conditions the hexagonal crystal axis c lies in the plane of the sample, so that we are interested in heat transfer in the direction perpendicular to the c axis. In the opposite case a most important role would be played by the substantial growth of $\tau(\mathbf{q})$ when the direction of $\mathbf{q}$ approaches the hexagonal axis of the crystal.[18]

We can thus separate two phonon groups of importance to us: thermal with energies $\hbar\omega \sim T$, whose distribution disequilibrium is determined by the inhomogeneous distribution of the temperature, and long-wave phonons propagating from the heated region almost ballistically. As we shall show, after times of the order of the observation time, the heating region is in the main localized at the front surface of the sample. This is reminiscent of the hot-spot picture proposed in Ref. 11 to explain experiments on dragging of EHD by thermal pulses. In contrast to Ref. 11, however, in our case the appearance of the hot spot is due to the contribution of the equilibrium-phonon system that causes the main mechanism of the phonon relaxation. The fact that the phonons of the main group are thermalized and propagate in the heat-conduction regime greatly facilitates the analysis of the disequilibrium of the phonon system compared with the low-temperature case (considered, in particular, in the papers of Levinson[20]).

In accord with the foregoing, the starting point for our problem is the equation for the temperature

$$\partial T/\partial t - \tilde{D}\nabla^2 T = 0, \qquad \tilde{D} = (2\pi^2/45)\bar{w}^2\tau_U, \qquad (2)$$

where $\tilde{D}$ is the thermal diffusivity coefficient. The boundary conditions for (2) are connected with the question of the heat dissipation. Estimates show that under conditions considered, over observation times $t \lesssim 10^{-7}$ sec, the heat dissipation can be neglected. We assume also that during this time the heat does not manage to propagate to the rear wall, so that the boundary conditions correspond to

$$\nabla T|_{x=0}=0, \quad \Delta T|_{x\to\infty}\to 0,$$

where $\Delta T = T - T_0$ and T_0 is the equilibrium temperature of the sample prior to irradiation.

We shall hereafter assume everywhere $\Delta T \ll T_0$, so that the parameters of the phonon and exciton systems can be regarded as given and the equations as linear. In this case the solution of (2) with δ-function initial conditions (injection of heat Q at the initial instant of time $t = 0$) is of the form

$$\Delta T = \frac{Q}{2\pi^{1/2} C (\tilde{D}t)^{1/2}} \exp\left(-\frac{x^2}{4\tilde{D}t}\right), \tag{3}$$

where C is the heat capacity of the phonon system. Recognizing that $\tilde{D} \approx 2\text{cm}^2/\text{sec}$, the heating region would reach the rear surface $x = L \approx 2\times 10^{-3}$ cm within a time $t \sim 10^{-6}$ sec, so that in an observation time $t < 10^{-7}$ sec we are indeed dealing with a hot spot localized on the front surface.

We turn now to the group of long-wave phonons responsible for the interaction with the excitons. The kinetic equation for the distribution function $N(\mathbf{q})$ of these phonons is of the form

$$\partial N/\partial t + \mathbf{w}\nabla N = \hat{I}N, \tag{4}$$

where $\hat{I}$ describes the interaction with the thermal phonons. Recognizing that this interaction should result in a Planck distribution function $N_0(T)$, as well as that the long-wave phonons constitute a small group in phase space, the term in question can be represented in the form

$$\hat{I}N = [N_0(T) - N]/\tau_*, \tag{4a}$$

where T is the local value of the temperature.

We begin the analysis of (4) and (4a) with the case $l_* = w\tau_* \gtrsim L$. Within the framework of the method of characteristics, the general solution of (4) can be represented in the form

$$N = \int_{\bar{t}_1}^{t} \frac{dt'}{\tau_*} N_0(T(t')) \exp\left(-\frac{t-t'}{\tau_*}\right), \tag{5}$$

where the integration is along the phonon trajectory and t' is the time that the phonon is located on the given point of the trajectory. For simplicity we neglect here the explicit dependence of T on the time, assuming that the time of spreading of the hot spot is much longer than the time of flight of the phonons. The constant $\bar{t}_1$ is determined from the boundary conditions on the surface of the sample. Assuming specular reflection we have $\bar{t}_1 = -\infty$ (the trajectory includes multiple reflection from the walls).

Since we assume $\hbar\omega \ll T$, it follows that

$$N_0(T) = T/\hbar\omega = (T_0 + \Delta T)/\hbar\omega.$$

The difference between N and the equilibrium distribution function is thus determined by the presence, in the integrand, of a term proportional to ΔT and different from zero only in the region of the hot spot at $x \lesssim (\tilde{D}t)^{1/2} \ll L$. The effect of interest to us is connected only with the flow part of the function N, which describes the directional flux of phonons, so that it is necessary to calculate the quantity

$$N^- = N(w_x > 0) - N(w_x < 0),$$

where w_x is the projection of the phonon velocity on x. Changing in (5) to integration with respect to the spatial variable ($dt' = dx/w_x$) and using (3) we obtain after simple transformations, for the function N^- inthe region outside the hot spot, i.e., at $x \gtrsim (\tilde{D}t)^{1/2}$, the following estimate:

$$N^- \approx \frac{Q}{C(\hbar\omega)} \frac{L-x}{L\tau_* w\cos\vartheta}, \tag{6}$$

where ϑ is the angle between w and the x axis; in accordance with the derivation conditions, $L/\cos\vartheta \ll w\tau_*$.

In the case of fully diffuse scattering of the phonons by the walls, we represent the general solution of (4) in the form

$$N = A\exp\left[-\frac{t-t_1}{\tau_*}\right] + \int_{t_1}^{t} \frac{dt'}{\tau_*} N_0(t') \exp\left[\frac{t'-t}{\tau_*}\right],$$

where the instant t_1 corresponds to the act of scattering by the wall (for phonons with $w_x > 0$ from the wall $x = 0$, for phonons with $w_x < 0$—from the wall $x = L$). The constant A is determined from the condition that the total phonon flux on the surface vanish. It can therefore be shown that the estimate of N^- in the region outside the hot spot takes the same form as in the case of specular scattering (6).

In the region of the hot spot, the order of magnitude of N^- agrees with the estimate (6), but the coordinate dependence ensures in this case vanishing of N^- at the wall $x = 0$.

In the case $l_* < L$, the solution of (4) can be obtained by the standard procedure of dividing N into parts symmetric and asymmetric in the velocities w, a procedure that leads to the diffusion equation. As a result, we have for N^- in the region outside the spot the estimate

$$N^- \approx \frac{Q}{C(\hbar\omega) w\tau_*} \exp\left(-\frac{x}{w\tau_*}\right). \tag{7}$$

We turn now to an investigation of the kinetics of the excitons. We use the standard Boltzmann kinetic equation for the exciton distribution function f. The exciton-phonon collision integral

$$\begin{aligned} \hat{I}_{ep} = \sum_{\mathbf{q}} M_{\mathbf{q}} \{ &[f_{\mathbf{p}+\hbar\mathbf{q}}(N_{\mathbf{q}}+1) - f_{\mathbf{p}} N_{\mathbf{q}}]\delta(\varepsilon_{\mathbf{p}+\hbar\mathbf{q}} - \varepsilon_{\mathbf{p}} - \hbar\omega_{\mathbf{q}}) \\ &+ [f_{\mathbf{p}-\hbar\mathbf{q}} N_{-\mathbf{q}} - f_{\mathbf{p}}(N_{-\mathbf{q}}+1)]\delta(\varepsilon_{\mathbf{p}-\hbar\mathbf{q}} - \varepsilon_{\mathbf{p}} + \hbar\omega_{\mathbf{q}})\} \end{aligned} \tag{8}$$

is of the same form as the usual electron-phonon collision integral (the difference is determined by the value of M_q). This is due, in particular, to the fact that in our case the characteristic phonon frequencies are much lower than the exciton excitation energy, and the characteristic wavelengths are much larger than the Bohr radius. We assume also that the wavelengths of the phonons that interact with the excitons are shorter than the mean free path of the excitons.

We now transform (8), separating the contributions of the symmetric and asymmetric (in $\mathbf{q}$) parts of the phonon distribution function $N_{\mathbf{q}}$. The contribution of the symmetric part N^+, determined in our approximation by the distribution function of the equilibrium phonons N_0, causes the usual relaxation of the exciton distribution function with a characteristic momentum relaxation time τ_p:

$$\hat{I}_{ep}{}^+ \equiv \hat{I}[N^+, f_{\mathbf{p}}] \sim f_{\mathbf{p}}/\tau_p.$$

Theoretical estimates lead to values $\tau_p \sim 10^{-12}$–10^{-13} sec, which agrees with experiment. On the other hand, the contribution of the part antisymmetric in $\mathbf{q}$ is transformed into (cf. REf. 21):

$$\dot{I}_{ep}^{-} = \sum_{\mathbf{q}} M_{\mathbf{q}} N_{\mathbf{q}}^{-} [f_{\mathbf{p}+\hbar\mathbf{q}} - f_{\mathbf{p}}] \\ [\delta(\varepsilon_{\mathbf{p}+\hbar\mathbf{q}} - \varepsilon_{\mathbf{p}} - \hbar\omega_{\mathbf{q}}) - \delta(\varepsilon_{\mathbf{p}+\hbar\mathbf{q}} - \varepsilon_{\mathbf{p}} + \hbar\omega_{\mathbf{q}})]. \quad (9)$$

It is easily seen that the operator $\hat{I}_{ep}$ changes the parity of the function f_p with respect to $\mathbf{p}$. We note that the contribution of the small q to (9) takes now the standard form of the kinetic-equation force term proportional to $\partial f/\partial \mathbf{p}$.

We shall assume hereafter throughout that the mean free path of the ecitons is much shorter than the characteristic spatial scales of the variation of f, and the rate of temporal variation of f is much less than τ_p. With these circumstances taken into account, using the standard Chapman-Enskog procedure, we arrive at a diffusion equation for the exciton density $n(x,t)$:

$$\frac{\partial n}{\partial t} - D\nabla^2 n + \mu \mathbf{F}\nabla n + \frac{n}{\tau} = 0, \quad (10)$$

where

$$D = {}^1/_3 \bar{v}^2 \tau_p, \qquad \mu = \tau_p/m.$$

The term proportional to $\mathbf{F}$ is connected with the contribution of the operator $\hat{I}_{ep}$ and describes the phonon dragging of the excitons. We can obtain for F the following estimate:

$$F \sim \frac{\bar{p}}{\tau_p}\frac{w}{\bar{v}}\left(\frac{|N^-|}{N_0}\right)_{\hbar\omega \sim Tw/\bar{v}}. \quad (11)$$

The dragging force F, proportional to the antisymmetrical part of the phonon distribution function N^-, depends generally speaking on the coordinates and on the time. In particular, it vanishes at the walls (cf. (6)). It can differ from the estimate that follows from (11) and (6) near the front wall—in the region of the hot spot and, in particular, in the region of absorption of the laser radiation. We shall, however, analyze next Eq. (10) under the assumption that F is constant. This approach makes it possible, in any case, to obtain order-of-magnitude estimates; its results can be used for a quantitative analysis of the situation when F is not constant if, nonetheless, the spatial and temporal changes of F are slower than the corresponding change of the solution of (10).

To solve Eq. (10) it is necessary to formulate boundary and initial conditions for it. We note first of all that, as mentioned earlier, the experimental results (primarily comparison of the data of Ref. 8 for the radiation on the FE and FE–*LO* lines) indicate that the surface acts as a region of effective recombination (see also Ref. 22). In this case, in particular, it has been established[8] that a noticeable decrease in the exciton density takes place near the surface within times $\tau_S \lesssim 10^{-9}$ sec substantially shorter than the time τ_V of the volume recombination. For a model description of this phenomenon we propose that near the surface there exists a layer of thickness d with a characteristic recombination time $\tau_S \ll \tau_V$ (the real presence of such a layer can be due to near-surface defects). If we assume $d \ll \alpha^{-1}$, it is easily seen that from the point of view of describing the considered effect this recombination source can be regarded as a pure surface source with a given recombination rate $v_r = d/\tau_S$ (so that the flux of the particles that recombine on the surface $x = 0$ is $j_r = v_r n$). In this situation, the surface density n is determined both by the surface recombination and by the influx of particles from the volume on account of diffusion. It is easy to show that if in this case (as a result of the action of the source) a certain exciton distribution was produced in the subsurface region, the decrease of the density n with time at $x = 0$ after turning off the source will follow a power law (if the initial distribution is homogeneous over the sample, this law corresponds to the asymptotic expression $n \propto (D/v_r^2 t)^{1/2}$). It follows from experiment that the shape of the FE-line emission pulse, in reflection geometry, duplicates almost exactly (within $\sim 10^{-9}$ sec) the shape of the laser pulse. To describe this behavior soley within the framework of surface recombination it is necessary to invoke values of V_r considerably larger than those which follow from estimates of the exciton surface density. These circumstances (as well as the behavior of the pulse on the FE–*LO* line) force us to assume that the relation $d > \alpha^{-1}$ is realized in the experiment.

Favoring the foregoing arguments are also the differences in the temporal kinetics of the luminescence observed at weak excitation intensities for different samples. Figure 6 shows schematically the characteristic time dependences of the radiation on the FE–*LO* line, as well as on the FE line, in reflection geometry for three groups of samples. For the samples of the first group (which are the most typical), at low excitation intensities, the shape of the pulse on the FE–*LO* line almost agrees with the shape of the laser pulse; the earlier experimental data were obtained precisely for such samples. For the samples of the second group, slow kinetics for the FE–*LO* line was observed already at small I. For the third group of samples, slow temporal kinetics appeared also on the FE line. The signal for the rear surface on the FE line (in the transmission geometry) for the samples of the third and second groups was noticeably stronger than for samples of the first group. This behavior can be easily explained by assuming that for the samples of the first group the condition $\alpha^{-1} < (D\tau_S)^{1/2} < d$ is satisfied, for the samples of the second group we have $\alpha^{-1} < d \lesssim (D\tau_S)^{1/} \gtrsim^2$, and for the third group $\alpha^{-1} \sim d \ll D\tau_S)^{1/2}$.

We assume in addition that the condition $d \ll (Dt_0)^{1/2}$ is satisfied, i.e., that the diffusion time in the given layer is much shorter than the characteristic times of the problem. This condition enables us to reduce the problem for a layer to a stationary problem whose solution, in turn, makes it possi-

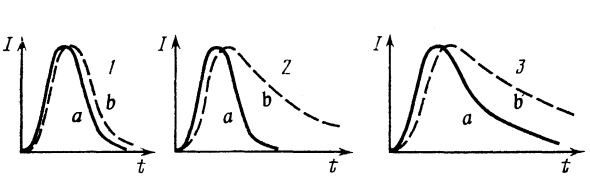

FIG. 6. Shape of luminescence pulse at $I = 10^{18}$–10^{19} cm^{-2}·sec^{-1} for the three groups of samples investigated in the experiment.

ble to formulate effective boundary conditions for Eq. (10). A natural distinction can be made here between two stages. In the first stage $t < t_0$, i.e., during the time of action of the laser pulse we have subsurface source of particles with a flux density $j_0 \sim N_e/t_0$, where N_e is the total number of produced excitons per square centimeter. Taking this factor into account, and also neglecting the purely surface recombination, we can show that on the layer boundary $x = d$ the density is[2)]

$$n_0 = j_0 \left(\frac{\mu^2 F^2 \tau_s + 4D}{4\tau_s}\right)^{-1/2} \exp\left\{-\frac{d}{D}\left[\left(\frac{\mu^2 F^2}{4} + \frac{D}{\tau_s}\right)^{1/2} - \frac{\mu F}{2}\right]\right\}, \tag{12}$$

i.e., at $\mu^2 F^2 \tau_s / 4D \ll 1$ we have

$$n_0 \sim j_0 \left(\frac{\tau_s}{D}\right)^{1/2} \exp\left\{-\frac{d}{(D\tau_s)^{1/2}}\left[1 - \frac{\mu F}{2}\left(\frac{\tau_s}{D}\right)^{1/2}\right]\right\},$$

and at $\mu^2 F^2 \tau_s / 4D \gg 1$ we have

$$n_0 \sim \frac{2j_0}{\mu F} \exp\left(-\frac{d}{\mu F \tau_s}\right).$$

Neglecting the layer thickness d compared with L, we use (12) as the boundary condition for (10) at $x = 0$ for the times $0 \leqslant t \leqslant t_0$; the initial conditions for (10) in this stage corresponds to $n|_{t=0} = 0$. We note that the discrepancy between the initial and boundary conditions at $x = 0$ is due to the fact that the matching of these conditions takes place in a narrow sub-surface layer, whose thickness we neglect. This discrepany is immaterial for the calculation that follows.

The second state $t > t_0$ characterizes the propagation of the produced exciton cloud in the absence of a source. The initial condition for this stage is determined by specifying the shape of the cloud at the instant $t = t_0$ (which, in turn, is determined from the solution for the preceding stage), and the boundary condition at $x = 0$ corresponds to the condition of effective recombination in the subsurface layer, i.e., $n|_{x=0, t>t_0} = 0$.

It can be shown (see the Appendix) that by solving the corresponding problem we arrive at the following estimates for the exciton density at the point $x = L$ for an instant $t > t_0$. At $\mu F \ll 4D/L$ (weak dragging) we have

$$n \sim \frac{n_0 L_0^3}{2\sqrt{\pi}} \frac{1}{(Dt)^{3/2}} e^{-t/\tau_V} e^{-L^2/4Dt}. \tag{13}$$

For strong dragging, when $4D/L < \mu F < 4DL/L_0^2$, we obtain

$$n \sim \frac{n_0 L_0}{2\sqrt{\pi}} \frac{1}{(Dt)^{1/2}} e^{-t/\tau_V} \exp\left[-\frac{(L-\mu F t)^2}{4Dt}\right], \tag{14}$$

and at $\mu F > 4DL/L_0^2$ we get

$$n \sim e^{-t/\tau_V} \tilde{n}(L - \mu F t). \tag{15}$$

Here L_0 is the characteristic initial dimension of the exciton cloud (at the instant of time $t = t_0$), and $\tilde{n}(x)$ is a function that describes the distribution of the excitons in the cloud at $t = t_0$. For L_0 we have the estimates

$$\begin{aligned} L_0 &\sim 2(Dt_0)^{1/2}, \quad \mu F \ll (4D/t_0)^{1/2}, \\ L_0 &\sim \mu F t_0, \quad \mu F \gg (4D/t_0)^{1/2}. \end{aligned} \tag{16}$$

We examine now how the results can be affected by the dependence of the force F on the coordinate and, in particular, by the vanishing of the force on the rear surface of the sample ($x = L$). It can be seen that in the case of strong dragging we are dealing with displacement of the exciton cloud with velocity $v = \mu F$, accompanied by its diffusion spreading (cf. (14)). Thus, if $F = F(x)$ and $v = v(x)$, the time of displacement of the cloud from the point $x = 0$ to the point $x = L$ is estimated at

$$\Delta t = \int_0^L dx/v(x).$$

Taking (6) and (11) into account, we have

$$v = v_0\left(\frac{L-x}{L}\right), \quad \Delta t \approx \frac{L}{v_0} \ln \frac{L}{\tilde{L}}.$$

Here $\tilde{L}$ is a certain length that determines the cutoff of the integration. Since this cutoff is determined by the diffusion spreading of the cloud, $\tilde{L}$ is estimated the equation

$$\tilde{L}^2/4D \sim (L/v_0)\ln(L/\tilde{L}). \tag{17}$$

Thus, the effect of vanishing of the force F on the rear surface reduces to a lengthening of the time of displacement of the cloud by a factor $1 + \ln(L/\tilde{L})$, corresponding to the following substitution in(14) and (15):

$$t \to \left(1 + \ln\frac{L}{\tilde{L}}\right)^{-1} t. \tag{18}$$

A behavior of this kind can be expected at $w\tau_* \gtrsim L$. If, however, the mean free path of the low-frequency phonons is shorter than L, the decrease of the force F (and accordingly of the drift velocity) at the rear wall becomes exponential (cf. (7)). Accordingly, the average drift velocity decreases exponentially with increasing parameter $L/w\tau_*$, namely

$$\bar{v} \sim v_0 \exp\left(-\frac{L}{w\tau_*}\right) \tag{19}$$

and in the case $L/w\tau_* > \ln(Lv_0/4D)$ the motion of the excitons becomes purely diffuse.

4. DISCUSSION OF RESULTS

We proceed to discuss the results and to compare the experimental data with the developed theory. We emphasize first that our theoretical description (based on a number of assumptions) claims to describe the main qualitative relations and tendencies, as well as order-of-magnitude estimates.

We begin with the experiment on the observation of the motion in a CdS sample, of FE produced in the region $x = 0$ and detected in the region $x = L$ (Fig. 5). The corresponding experimental data and the results of the calculation of the temporal profiles of the exciton luminescence on the basis of (14) are shown in Fig. 7. When comparing the theoretical curves with experiment, the adjusting parameter employed was the drift velocity $V_{dr} = \mu F$. The values of V_{dr} obtained in this manner lie in the range 10^4–10^5 cm/sec; this agrees with the argument that the maximum velocity of the dragged excitons must not exceed that of sound $\overline{w} = 3.5 \times 10^5$ cm/sec (Ref. 23). It can be seen that, in the main, the theoretical

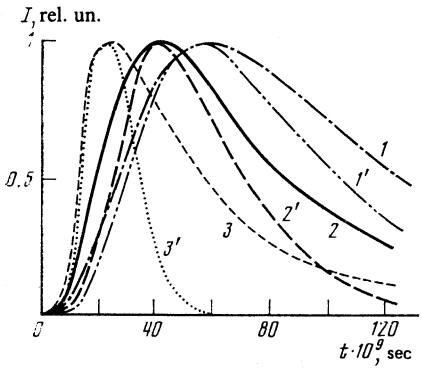

FIG. 7. Comparison of the observed shape of the radiation pulse of FE in the geometry $\mathbf{k}_I \| \mathbf{k}_L$ with that calculated from (14): $T = 77$ K, $L = 2\times10^{-3}$ cm: 1—$I = 1.2\times10^{23}$ cm^{-2}·sec^{-1}, 2—$I = 8\times10^{23}$ cm^{-2}·sec^{-1}, 3—$I = 4\times10^{24}$ cm^{-2}·sec^{-1}; calculation in accordance with (14) for $T - v_{dr} = 8\times10^3$ cm/sec 2'—$v_{dr} = 3\times10^4$ cm/sec; 3'—$v_{dr} = 8\times10^4$ cm/sec.

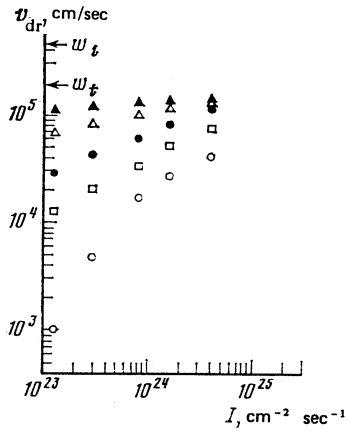

FIG. 8. Dependence of the FE drift velocity on the excitation intensity and on the temperature (▲—40 K, △—60 K, ●—80 K, □—120 K, ○—130 K)

curves describe correctly the qualitative picture (the shift of the maximum and the decrease of the half-width of the pulse with increasing pump). For weak pumps, the agreement between the theoretical and experimental curves is quite good. With increasing excitation intensity, however, a certain time lag of the luminescence signal is observed compared with the theory. The observed discrepancies can be due, as indicated in Sec. 3, to the fact that the dragging force, and hence the drift velocity, is not constant over the crystal (as was assumed in the derivation of (14)), but vanish at the surface. This leads to a certain spreading of the profile of the signal at the detector at $x = L$ ($\mathbf{k}_I \| \mathbf{k}_L$) in accordance with (14) and (18). We shall discuss also the role of another restriction of the theory ($\Delta T \ll T$) in the derivation of (14). As noted above, the temperature rise ΔT is localized in a narrow subsurface region of the hot spot, whereas the bulk of the sample does not manage to become heated during the time of the experiment. Therefore when analyzing the exciton transport in the bulk of the sample we can assume the temperature to be constant and thus, dispense with the restriction $\Delta T \ll T$ in the derivation of (14). All that matters for this derivation is the presence, in the interior of the sample, of a drift force F which we assume in the derivation of (14) to be given (and for simplicity, independent of the coordinate). With the foregoing taken into account, the use of (14) for the analysis of the experimental curves is justified in a wide range of excitation intensities.

It is convenient to reduce the experimental results and to plot the funciton $v_{dr} = f(I)$ with the aid of the analytic expression for Δt_{max}, which is the time interval between the signals from the regions $x = 0(\mathbf{k}_I \| -\mathbf{k}_L)$ and $x = L$ ($\mathbf{k}_I \| \mathbf{k}_L$); this expression is obtained from the extremum condition for (14);

$$\Delta t_{max} = -\frac{D\tau_v}{4D+\tau_v v_{dr}^2} + \left[\left(\frac{D\tau_v}{4D+\tau_v v_{dr}^2}\right)^2 + \frac{L^2\tau_v}{4D+\tau_v v_{dr}^2}\right]^{1/2}. \quad (20)$$

It can be seen that the drift prevails over diffusion if $D < \tau_v v_{dr}^2$. In the caser $T = 80$ K, $D = 7$ cm^2/sec, and $\tau_v \sim 10^{-8}$ sec we obtain the estimate $v_{dr} \gtrsim 10^4$ cm/sec, which agrees with the experimental situation.

We have investigated the dependences of v_{dr}, defined in accordance with (20), on the temperature and on the pump intensity I. The results are shown in Fig. 8. From the analysis of the corresponding $v_{dr} = f(I,T)$ curves of Fig. 8 it can be seen that at relatively high temperatures and weak pumping $I \sim 10^{23}$ cm^{-2}·sec^{-1} the velocity v_{dr} depends linearly on I. At $I \sim 10^{24}$ cm^{-2}·sec^{-1} the $v_{dr}(I)$ dependence becomes sublinear and saturates. Attention must be called to the fact that with decreasing temperature the linearity region decreases (accordingly, the lengths of the saturation region increases), thus indicating an increase of the effectiveness of the dragging with decreasing temperature. These facts, in conunction with $v_{dr} \lesssim 10^5$ cm/sec, are arguments in favor of the phonon mechanism of dragging and agree with the deductions of the theory.

In the preceding arguments we have in fact not discussed the nature of v_{dr}; this quantity was used only as a parameter that determines the kinetics of the excitons. We now compare the values and dependences obtained for this quantity from an analysis of the experiment, with a theoretical calculation that takes into account the behavior of the phonon system in accordance with (6), (7), and (11). Inasmuch as within the framework of this calculation we have invoked the hotspot region (which serves as the source of nonequilibrium phonons), the restriction $\Delta T \ll T$ turns out to be quite significant. Therefore estimates of F and v_{dr} were obtained under the assumption $\Delta T \ll T$ and correspond in fact to a linear $v_{dr} = f(I)$ dependence, i.e., they are valid only in the region of small I. A numerical comparison of the conclusions of the theory with experiment will therefore be made precisely for this region. As follows from (11) and (19), the estimate for v_{dr} is expressed in the form

$$l_* = w\tau_* \gtrsim L, \quad v_{dr} \approx v_0 \approx wQ/CTl_*, \quad (21a)$$

$$l_* \lesssim L, \quad v_{dr} \approx v_0 \exp(-L/l_*). \quad (22b)$$

The heat capacity of CdS crystals can be obtained from an analysis of the data of Ref. 24: We have $C \approx 6\times10^{21}$ cm^{-3} at $T \approx 50$ K. Then, in accordance with (21a), putting $Q \approx 8\times10^3$ erg/cm^2 (which corresponds to $I \approx 10^{23}$

$cm^{-2}\cdot sec^{-2}$ and $t_0 \sim 10^{-8}$ sec), we obtain at $T \approx 50$ K the value $v_{dr} \approx 3 \times 10^4$ cm/sec; this estimate agrees with the experimental value of v_{dr} (Fig. 7). The theory describes satisfactory also the observed temperature dependence. In fact, in the experiment the value of v_{dr} drops steeply when the temperature is raised from 80 to 130 K (from 3×10^4 to 1.7×10^3 cm/sec). As can be seen from (21b), this behavior takes place if $l_* \lesssim L$; in this case v_{dr} decreases exponentially with decreasing l_*, whereas l_* in turn decreases with increasing T like T^{-3} (1). From an analysis of the $v_{dr}(T)$ dependence we can conclude that l_* becomes equal to L at $T \approx 100$ K.

We turn now to an analysis of the surface kinetics. As noted above, the time dependences of the luminescence in reflection geometry suggest that $\tau_S \lesssim 10^{-9}$ sec and $d \sim (D\tau_S)^{1/2} \approx 0.8 \times 10^{-4}$ cm. In accordance with the estimates (12), in the case of sufficiently effective drift (when $\mu F \gtrsim 2(D/\tau_S)^{1/2}$, the subsurface density ceases to increase linearly with increasing I. On the other hand, in this situation the excitons penetrate effectively into the interior of the crystal, and when account is taken of (16) the total number of excitons penetrating into the volume depends linearly on I. This explains both the sublinear dependence of the luminescence on the FE line with incresing $I$and the behavior of the phonon-replica pulse (Fig. 1–3). An estimate of the drift velocity, starting with which this behavior comes into play, corresponds to 10^5 cm/sec, in satisfactory agreement with experiment.

We turn finally to the question of the temperature of the subsurface region of the crystal, which serves as the injector of long-wave phonons, and to the time evolution of the hot spot. An estimate of the temperature rise in this region $\Delta T \approx (Q/2C)(Dt)^{1/2}$ yields at $I \sim 10^{23}$ $cm^{-2}\cdot sec^{-1}$ a value $\Delta T \approx 5$ K, and at $I \sim 10^{24}$ cm^{-2} sec^{-1} one obtains $\Delta T \approx 25$ K.[3)] In this case, during the characteristic times of the experiment, the hot spot propagates over a distance $x \lesssim 6 \times 10^{-4}$ cm.

We call attention to the fact that if we use the known data on the influence of the temperature on the luminescence spectrum, then when account is taken of the estimated ΔT, one might expect a spectral shift of the recombination-radiation lines at sufficiently large I. In experiment, however, no such shift is observed. This disparity, in our opinion, can be due to the fact that the indicated temperature dependences of the spectrum were obtained, generally speaking, under the conditions of homogeneous quasistationary heating. In the situation investigated, however, we have on the one hand a substantial inhomogeneity (the region of the hot spot is bounded by unheated sections of the sample and this modifies in particular the character of the thermal expansion). On the other hand, the heating is not stationary, and we have seen that the phonon system, at any rate in the long-wave part of the spectrum, remains essentially in disequilibrium. We hope to analyze this question in succeeding studies.

CONCLUSION

1. We observed and investigated the dragging of free excitons by nonequilibrium acoustic phonons generated in nonradiative recombination and thermalization of NEHP in the subsurface layer of a crystal. A theory of this phenomenon was constructed and takes into account phonon-phonon processes with participationof equilibrium phonons. Because of these processes, the bulk of the phonons turns out to be thermalized, and near the surface there is produced an increased-temperature region (hot spot) that expands by heat conduction. Interacting with the excitons, however, are long-wave phonons whose propagation is close to ballistic; the hot spot plays a role of an injector of such phonons. It is shown that the exciton drift velocity in this situation reaches saturation with increasing pump intensity, and at $I \sim 10^{24}$ $cm^{-2}\cdot sec^{-1}$ its value is $\sim 10^5$ cm/sec, i.e., close to the speed of sound. We investigated the dependences of v_{dr} on the temperature and on the intensity of the optical excitation. We investigated the dragging of excitons by low-energy phonons of a thermal pulse obtained by heating with a laser pulse a metal film deposited on the surface of a sample.

2. It is shown that the observed changes in the recombination-radiation spectrum of an electron-hole system of direct-band semiconductors at high optical-excitation intensity in the region of the phonon replicas of a free exciton can be attributed to a change of the spatial distribution of the NEHP in the sample, due to the dragging of the excitons by nonequilibrium acoustic phonons.

3. The possibility was demonstrated of investigating processes in a phonon system with the aid of optical methods. The procedure employed has high spatial, spectral, and temporal resolution and can turn out to be quite fruitful. As a result of an investigation of the interaction of excitons with acoustic phonons and comparison of the result with the developed theory, information was obtained in the form of the distribution function and of the mean free paths of long-wave phonons. The mean free path of phonons of energy $\sim 10^{-3}$ eV turns out to be of the order of 10^{-3} cm at $T \approx 100$ K.

4. It is shown that study of the processes of dragging of excitons by phonons yields information on the kinetics of excitons in the subsurface region, particularly on the spatial dependence of the recombination time.

We thank O. N. Talenskiĭ for supplying the CdS samples, U. Parmanbekov for help with the measurements, and Yu. M. Gal'perin, V. L. Gurevich, E. L. Ivchenko, and Yu. V. Pogorel'skiĭ for a discussion of the work and for a number of valuable remarks and suggestions.

APPENDIX

The general solution of (10), defined on the entire real axis and corresponding to the initial-condition problem, can be represented in the form

$$n = \frac{1}{2\pi^{1/2}} e^{-t/\tau_v} \int_{-\infty}^{+\infty} \frac{\varphi(\xi)}{(Dt)^{1/2}} \exp\left[-\frac{(x-\xi-\mu Ft)^2}{4Dt}\right] d\xi, \quad \text{(A.1)}$$

where

$$\varphi(x) = n(x, t)\,|_{t=0}.$$

In our case only the region $x \geqslant 0$ has physical meaning; at the same time, for the first stage of the development of the exciton cloud, $0 \leqslant t \leqslant t_0$, we deal not with a nonzero initial condi-

tion but with the boundary condition defined by (12). We use the solution (A.1), defining additionally $\varphi(\xi)$ also for the region $\xi<0$; this enables us to reduce the boundary condition at $x=0$ to a certain initial condition at $t=0$ for the region $x<0$. On the basis of (13) we can represent the boundary condition (12) in the form

$$n|_{x=0}=\frac{1}{2\pi^{1/2}}e^{-t/\tau_V}\int_{-\infty}^{0}\frac{\varphi(\xi)}{(Dt)^{1/2}}\exp\left[-\frac{(\xi+\mu Ft)^2}{4Dt}\right]d\xi=n_0, \quad \text{(A.2)}$$

which is an integral equation for $\varphi(\xi)$. Assuming that $t_0\ll\tau_V$, we obtain an order-of-magnitude estimate $\varphi\sim n_0$. Starting from (A.1 and A.2) we can obtain

$$n\approx n_0\left\{1-\frac{1}{\pi^{1/2}}\int_0^{x/(Dt)^{1/2}}C(u)\exp\left[-\left(u-\frac{\mu F}{2}\left(\frac{t}{D}\right)^{1/2}\right)^2\right]du\right\}, \quad \text{(A.3.)}$$

where $C\sim 1$ depends little on u, with

$$\frac{1}{\sqrt{\pi}}\int_0^{\infty}C(u)\exp\left[-\left(u-\frac{\mu F}{2}\left(\frac{t}{D}\right)^{1/2}\right)^2\right]du=1.$$

It can be seen from the obtained expressions that at the instant when the laser pulse stops the distribution of the excitons can be described by the following interpolation formula:

$$n(t_0)\sim n_0\left[\exp\left(\frac{x-\mu Ft_0}{2(Dt_0)^{1/2}}\right)+1\right]^{-1}. \quad \text{(A.4)}$$

It corresponds to an exciton cloud whose dimensions in the case of weak dragging, i.e., at $(\mu F)^2\ll 4D/t_0$, is of the order of $2(Dt_0)^{1/2}$, and for strong dragging, i.e., at $(\mu F)^2\gg 4D/t_0$, of the order of μFt_0.

The second stage corresponds to propagation of an exciton cloud in the absence of a source. The initial condition for this part of the problem is the distribution (A.3), (A.4). The boundary condition is that effective recombination occur in a thin subsurface layer $x\leqslant d$. With account taken of the statement made in Sec. 3 above, it can be reduced in the case $D\tau_S^2/d^2t_0\ll 1$ to the condition $n|_{x=0}=0$ (just as before, the joining together of the boundary and initial conditions takes place in the subsurface layer, in which we are not interested). We note that this is precisely the stage that determines the slow luminescence kineticts connected, in particular, with the transport of excitons to the rear surface. To solve the problem during this stage we use again the general solution (A.1). It is easily seen that the boundary condition $n|_{x=0}=0$ can be satisfied by defining $\varphi(\xi<0)$ in (A.1) in such a way that $\varphi\exp(-\mu F\xi/2D)$ is continued into this region in odd fashion. Taking the foregoing into account, we obtain after simple transformations at $t\gg t_0$

$$n=\frac{1}{2\pi^{1/2}}e^{-t/\tau_V}\int_0^{\infty}\frac{\tilde{n}(\xi)}{(Dt)^{1/2}}\left[\exp\left\{-\frac{(x-\xi-\mu Ft)^2}{4Dt}\right\}-\exp\left\{-\frac{(x+\xi+\mu Ft)^2}{4Dt}\right\}\right]d\xi, \quad \text{(A.5)}$$

where $n(x)$ is defined in accordance with (A.3) and (A.4). Analyzing (A.5) in different limiting situations, we arrive at the estimates (13)–(15).

[1)]We note that the relations given here correspond to typical samples. In Sec. 3 we present also certain data concerning the variation of the observed dependences for different samples, discuss in greater detail the character of the recombination in the system, and advance additional arguments favoring our point of view.

[2)]Strictly speaking, we have calculated before the phonon distribution function N and thus also the force F only for $t>t_0$. It can be seen, however, for order-of-magnitude results that these estimates can be used also at $t\sim t_0$. We note also that for F in (12) it is necessary to use its characteristic value in the subsurface layer $x\lesssim d$.

[3)]It must be emphasized that the region of applicability of our theory is limited by the requirement $\Delta T\ll T$. As seen from Fig. 8 this condition (and consequently also the validity of our estimates) is violated at $I\geqslant 10^{24}$ $\text{cm}^{-2}\cdot\text{sec}^{-1}$.

[1]C. Klingshirn and H. Haug, Phys. Rept. **70**, 315 (1981).
[2]C. B. a la Guillaume, J. M. Debever, and F. Salvan, Phys. Rev. **177**, 567 (1969).
[3]V. G. Lysenko, V. I. Revenko, T. G. Tratas, and V. B. Timofeev, Zh. Eksp. Teor. Fiz. **68**, 335 (1975) [Sov. Phys. JETP **41**, 163 (1975)].
[4]R. F. Lehney, J. Shah, and C. C. Chiang, Sol. St. Commun. **25**, 621 (1978).
[5]H. Saito, S. Hionoya, and E. Hanamura, *ibid.* **12**, 227 (1973).
[6]B. S. Razbirin, I. N. Ural'tsev, and G. V. Mikhailov, Pis'ma Zh. Eksp. Teor. Fiz. **25**, 191 (1977) [JETP Lett. **25**, 174 (1977)].
[7]L. A. Kulevsky and A. M. Prokhorov, IEEE, **QI-2**, No. 9, 584 (1966).
[8]N. N. Zinov'ev and N. D. Yaroshetskiĭ, Fiz. Tekh. Poluprov. **14**, 464 (1980) [Sov. Phys. Semicond. **14**, 274 (1980)]. N. N. Zinov'ev and I. D. Yaroshetskiĭ, Pis'ma Zh. Eksp. Teor. Fiz. **33**, 109 (1981). [JETP Lett. **33**, 103 (1981)]. N. N. Ziov'ev, U. Parmanbekov, and I. D. Yaroshetskiĭ, Fiz. Tekh. Poluprov. **16**, 240 (1982) [Sov. Phys. Semicond. **16**, 150 (1982)].
[9]L. V. Keldysh, Pis'ma Zh. Eksp. Teor. Fiz. **23**, 100 (1976). [JETP Lett. **23**, 86 (1976)]. V. S. Bagaev, L. V. Keldysh, N. N. Sibel'din, and V. A. Tsvetkov, Zh. Eksp. Teor. Fiz. **70**, 702 (1976). [Sov. Phys. JETP **43**, 362 (1976)].
[10]a) N. N. Zinovev, U. Paramanbekov, and I. D. Yaroshetskiĭ Pis'ma Zh. Eksp. Teor. Fiz. **33**, 601 (1981) [JETP Lett. **33**, 584 (1981)]. b) N. N. Zinov'ev, L. P. Ivanov, I. G. Lang, S. T. Pavlov, A. V. Prokanikov, and I. D. Yaroshetskiĭ, Pis'ma Zh. Eksp. Teor. Fiz. **36**, 12 (1982) [JETP Let. **36**, 14 (1982)].
[11]J. C. Hensel and R. C. Dynes, Phys. Rev. Lett. **39**, 969 (1977).
[12]M. Greenstein and J. P. Wolf, Phys. Rev. B **24**, 3318 (1981).
[13]W. P. Dumke, Phys. Rev. **105**, 139 (1957).
[14]M. S. Epifanov, E. A. Bobrova, and G. N. Galkin, Fiz. Tekh. Poluprov. **9**, 1529 (1975) [Sov. Phys. Semicond. **9**, 1008 (1975)].
[15]É. L. Nolle, Fiz. Tverd. Tela (Leningrad) **9**, 122 (1967) [Sov. Phys. Solid State **9**, 20 (1967)].
[16]S. Modesti, A. Frova, J. L. Staehli, M. Guzzi, and M. Capizzi, Phys. Stat. Sol. (b) **108**, 281 (1981).
[17]W. E. Bron, Rept. Prog. Phys. **43**, 301 (1980).
[18]V. L. Gurevich, Kinetika fononnykh sistem (Kinetics of Phonon Systems), Nauka, 1980.
[19]G. E. Moore and M. V. Klein, Phys. Rev. **179**, 722 (1969).
[20]I. B. Levinson, Zh. Eksp. Teor. Fiz. **79**, 1394 (1980) [Sov. Phys. JETP **52**, 704 (1980)].
[21]A. I. Ansel'm, Vvedenie v teoriyu poluprovodnikov (Introduction to the Theory of Semiconductors), Nauka, 1978, p. 557.
[22]G. E. Pikus Osnovy teorii poluprovodnikovykh priborov (Principles of the Theory of Semiconducting Devices), Nauka, 1965.
[23]D. Berlincourt, H. Jaffe, and L. R. Shiozawa, Phys. Rev. **129**, 1009 (1963).
[24]K. Clusius and P. Harteck, Z. Phys. Chem. **134**, 243 (1928).

Translated by J. G. Adashko